Geochimica et Cosmochimica Acta Vol. 54, pp. 1217–1232

0016-7037/90/$3.00 + .00

Kamacite and olivine in ordinary chondrites: Intergroup and intragroup relationships

ALAN E. RUBIN
Institute of Geophysics and Planetary Physics, University of California, Los Angeles, CA 90024, USA

(*Received September* 22, 1989; *accepted in revised form February* 6, 1990)

Abstract—A suite of 134 ordinary chondrites (OCs) was analyzed by electron microprobe to determine olivine and kamacite compositions. Equilibrated members of the three main OC groups have the following ranges of olivine Fa and kamacite Co: H (17.3–20.2 mol% Fa; 4.4–5.1 mg/g Co); L (23.0–25.8 mol% Fa; 7.0–9.5 mg/g Co); LL (26.6–32.4 mol% Fa; 14.2–370 mg/g Co). However, the high-Co (200–370 mg/g Co) metal phase in highly oxidized LL chondrites is probably not kamacite. Group ranges of kamacite Ni content overlap, but mean Ni values of equilibrated OCs decrease from H (69.2 mg/g) to L (65.4 mg/g) to LL (49.8 mg/g). The concomitant increase in kamacite Co and decrease in kamacite Ni in the H-L-LL sequence is probably due to a combination of two effects: (1) the decrease in kamacite grain size from H through LL (the smaller LL grains reach equilibrium faster and thereby acquire lower Ni contents), and (2) the greater oxidizability of Fe relative to Co (kamacite grains thus become richer in Co as the oxidation state increases from H through LL).

There are significant intragroup differences in olivine and kamacite composition: type-3 and type-4 OCs tend to have lower olivine Fa and kamacite Co and Ni values than type-6 OCs. The lower Fa in H-L-LL3 chondrites may be due either to the lack of equilibration between fine FeO-rich and coarse FeO-poor silicates in type-3 OCs, or to the acquisition of less FeO-rich material (possibly type-II chondrules or fine-grained matrix material) by type-3 OCs during agglomeration. The lower kamacite Co and Ni contents of H-L-LL3 chondrites may reflect the presence in type-3 OCs of a relict nebular metal component with positively correlated Co and Ni; such a component has previously been inferred for the primitive, ungrouped chondrites, Al Rais, Renazzo, and ALH85085.

Aberrant olivine and/or kamacite grains with compositions significantly different than the majority in the whole-rock occur in at least half and probably virtually all equilibrated OCs. Aberrant kamacite grains are not uniformly distributed among the OCs; they are more common in L and LL than in H chondrites. Chondrites containing aberrant grains are fragmental breccias that were brecciated after cooling from high metamorphic temperatures.

The different OC parent bodies accreted at different heliocentric distances and acquired distinct bulk and mineralogical compositions. It is probable that more than three OC parent bodies were formed: Netschaevo is from an OC body more reduced than H chondrites; Tieschitz and Bremervörde may be from an OC body intermediate in its properties between H and L chondrites; and ten other OCs may be from a body intermediate between L and LL.

Within each individual OC group, there are many chondrites with non-overlapping olivine compositional distributions. These meteorites clearly have not equilibrated with each other; they may have agglomerated at opposite extremes of the parent body's accretion zone. Their existence is consistent with maximum metamorphic temperatures having occurred in small planetesimals prior to the accretion of large asteroids.

INTRODUCTION

THE THREE PRINCIPAL GROUPS of ordinary chondrites (OCs), H (high total Fe), L (low total Fe), and LL (low total Fe, low metallic Fe), constitute ~80% of all meteorites observed to fall. In going from H to L to LL chondrites, the abundances of siderophile elements decrease and the degree of oxidation increases. The proportion of oxidized Fe (i.e., FeO in silicates) increases at the expense of metallic Fe. Because Fe is more readily oxidized than Ni or Co, bulk metal becomes increasingly rich in Ni and Co (e.g., PRIOR, 1916). Equilibrated LL chondrites are thus characterized by high FeO/(FeO + MgO) ratios in olivine and low-Ca pyroxene, high taenite/kamacite ratios, and the occurrence of Co-rich kamacite.

KEIL and FREDRIKSSON (1964) and FREDRIKSSON et al. (1968) specified the compositional ranges of fayalite (Fa) in olivine and ferrosilite (Fs) in low-Ca pyroxene in equilibrated H, L, and LL chondrites; these values were later up-dated by GOMES and KEIL (1980). Because olivine equilibrates more rapidly than pyroxene (e.g., FREER, 1981), olivine data are more useful in establishing the degree of oxidation of type 3.7–4 OCs; for type-5 and type-6 OCs, olivine and low-Ca pyroxene data are equally useful.

SEARS and AXON (1976) and AFIATTALAB and WASSON (1980) specified the compositional ranges of Co concentrations in OC kamacite.

Olivine and kamacite data can aid in the classification of the vast majority of OCs independent of bulk compositional data. Nevertheless, there are some exceptions. In highly unequilibrated OCs (i.e., those of petrologic type ≤3.6; SEARS et al., 1980) olivine is too heterogeneous to yield meaningful mean fayalite values and in severely shocked OCs (e.g., those of shock facies e or f; DODD and JAROSEWICH, 1979) much of the metallic Fe-Ni may have been transformed into martensite.

The present study reports high-precision electron microprobe analyses of olivine and kamacite in a large suite of OCs. The purpose of the study was sixfold: (1) rigorously define the compositional ranges of these phases for each OC group, (2) identify anomalous OCs whose olivine and/or kamacite compositions lie outside the established ranges, and hence may not belong to the three main OC groups, (3) characterize the phases in the chondritic clasts of the Netschaevo iron meteorite and determine how closely related Netschaevo is to OCs, (4) determine if there are intragroup variations of olivine and kamacite compositions with petrologic type, (5) identify those OCs as fragmental breccias that contain some olivine and/or kamacite grains with aberrant compositions, and (6) search for new metallic Fe-Ni phases with extreme compositions. An expected by-product of this investigation was that a few meteorites that previously had not been well-characterized would be reclassified.

ANALYTICAL PROCEDURES

Olivine compositions were determined with the UCLA automated ARL-EMX electron microprobe using crystal spectrometers, two natural terrestrial olivine standards (with compositions of Fa 11.8 and Fa 17.9 mol%), 20-s counting times, standard correction procedures (BENCE and ALBEE, 1968), and a sample current of 15 nA at 15 keV. The precision is ±0.2 mol% Fa determined by repeated analyses of the standards. For most meteorites, 10–20 olivine grains were analyzed; analyses were made near grain centers. Low-Ca pyroxene in Netschaevo was analyzed following these same procedures.

Kamacite compositions were determined with the UCLA automated Cameca "Camebax-microbeam" electron microprobe using crystal spectrometers, 20-s counting times, ZAF corrections, and a sample current ranging from 10 to 15 nA at 20 keV. (On any given day, the beam current regulator maintained a constant current.) The standards were pure Fe metal, the kamacite of the Filomena hexahedrite for Ni (56.5 mg/g), and NBS steel 1156 for Co (73 mg/g). Kamacite from the Enshi H5 chondrite, averaging 4.5 mg/g Co, was analyzed in every run as an auxiliary standard; analyses of Enshi kamacite show that the precision in this range of Co concentration is ±0.1 mg/g Co. Six points were analyzed on the Fe standard and 15 points each were analyzed on the Co and Ni standards; care was taken to avoid phosphides in Filomena. Cobalt background counts were taken at wavelengths of 177.4 and 180.8 pm; these wavelengths were found to be the best suited for the elimination of the contribution of the Fe K_β peak to the Co K_α peak.

In most cases, 12 kamacite grains were analyzed in each meteorite; the main exceptions are the highly oxidized LL chondrites, in which kamacite is rare. Grains with ≥77.0 mg/g Ni were excluded because they are probably martensite (see below). Typically, two to three points were analyzed on the first two kamacite grains in each meteorite; if these grains were found to have similar compositions, then only one or two points were analyzed on additional grains if they also were found to have similar compositions. At least one analysis was made in the vicinity of the center of every analyzed grain. At least three points were analyzed on heterogeneous grains and grains with aberrant compositions relative to the majority.

In the most oxidized LL chondrites, high-Co, low-Ni metal grains were located by scanning the interfaces between high-Ni metal (tetrataenite or awaruite) and sulfide (troilite or pentlandite) with the Cameca loudspeaker tuned to the Co K_α wavelength.

Back-scattered electron and Mg, S, Fe, Ni, and Co X-ray images were made with the Cameca electron microprobe.

Some of the olivine Fa and kamacite Co data have been reported elsewhere (WANG and RUBIN, 1987; RUBIN et al., 1988; KALLEMEYN et al., 1989).

RESULTS

Compositional ranges and chondrite classification

The suite of 134 OCs in this study comprises 114 falls and 20 finds (Table 1). In general, the finds are not badly weathered; the sole exceptions are Artracoona, Brownfield (1937), and Pierceville, in which all of the metal has been oxidized. Meteorites from each group/type combination (i.e., H3–6, L3–6, LL3–6) were included. Most samples were selected because they were observed falls; in addition, several high-Fa LL chondrites were intentionally selected, and 11 meteorites that were classified by GRAHAM et al. (1985) as L chondrites (i.e., Artracoona, Borkut, Denver, Inman, Monte Milone, Peetz, Pierceville, Richmond, Sultanpur, Tathlith, and Trysil) were chosen because their U, Th-He ages are ≥3.2 Ga higher than those of most L chondrites (J. T. WASSON, pers. comm.).

Olivine was analyzed in every type 3.7–6 chondrite; the type ≤3.6 chondrites have very heterogeneous olivine and do not yield meaningful mean fayalite values (e.g., olivines in LL3.6 Parnallee range continuously from Fa 10.2 to 30.1). Kamacite was analyzed in virtually every chondrite including type ≤3.6 samples. Because the diffusion of Fe and Ni in metal is more rapid than the diffusion of Fe and Mg in olivine at a given temperature (AFIATTALAB and WASSON, 1980), meaningful mean kamacite Co and Ni values can be determined in many highly unequilibrated OCs.

Three meteorites (Jartai, Paragould, and Rose City) were found to contain no metallic Fe-Ni with ≤77 mg/g Ni (i.e., no kamacite) (Table 2); every low-Ni metal grain in these meteorites is in the compositional range of martensite and exhibits a martensitic structure when etched with nital. All three chondrites are significantly shocked; their shock facies (DODD and JAROSEWICH, 1979) range from d to f (KALLEMEYN et al., 1989), corresponding to equilibrium shock pressures of 20–80 GPa (STÖFFLER et al., 1988). Rose City is an impact-melt breccia (MASON and WIIK, 1966; FRULAND, 1975; RUBIN, 1985). The intense shock experienced by these meteorites has significantly altered their metal compositions (e.g., TAYLOR and HEYMANN, 1969). All three chondrites are excluded below from the chondrite group means of olivine and kamacite compositions.

Martensite (considered here to be metal with ≥77 mg/g Ni) was identified in a total of 34 chondrites, including meteorites from every group and petrologic type. In some chondrites (e.g., Guangnan) only one martensite grain was encountered; in others (e.g., Rose City) martensite occurs to the exclusion of kamacite. The proportion of martensite varies with chondrite group: H (14%), L (35%), and LL (22%). Bremervörde (designated H/L) also contains rare martensite grains. In addition, 4 out of 10 chondrites designated L/LL (see below) contain martensite (i.e., Knyahinya, Qidong, Sultanpur, and Xi Ujimgin); in Qidong and Xi Ujimgin, martensite is much more abundant than kamacite.

The range of olivine (in mol% Fa) in equilibrated OCs (Fa 17.3–32.4; Table 1) is comparable in width to that of terrestrial ultramafic rocks (Fa 7–22; DEER et al., 1982). The range of olivine Fa in the individual OC groups is much narrower: H4–6 (17.3–20.2), L4–6 (23.0–25.8), LL4–6 (26.6–32.4).

The range of the Co content of low-Ni metal in the OCs is very large [4.4–370 mg/g (Table 1)]; however, in the H and L chondrite groups, the kamacite range is quite narrow (4.4–5.1 and 6.7–9.5 mg/g Co, respectively). The large compositional range in LL chondrites (14.2–370 mg/g Co) mainly reflects the occurrence of very Co-rich phases (with ≥200

Table 1. Mean values and standard deviations of olivine Fa and kamacite Co and Ni in ordinary chondrites.

		Fa (mol%)			Co (mg/g)			Ni (mg/g)	
meteorite	type	n	mean	σ	n	mean	σ	mean	σ
Netschaevo*	HH6	10	14.3	0.3	12	4.5	0.3	66.4	1.7
Brownfield '37*	H3.7	10	18.4	0.3					
Dhajala	H3.8	20	19.3	0.3	12	4.8	0.3	67.4	4.0
Fleming*	H3.7	9	16.5	0.2	12	4.4	0.2	66.4	6.1
Grady (1937)*	H3.7	10	15.3	0.3	14	4.4	0.2	67.9	3.2
Laundry East*	H3.7	8	18.4	0.3	12	4.6	0.2	57.5	6.9
Prarie Dog Creek*	H3.6				9	4.5	0.1	70.6	3.1
Sharps	H3.4				12	4.7	0.7	70.3	4.5
Avanhandava	H4	10	18.0	0.2	12	4.5	0.2	71.2	0.5
Beaver Creek	H4	10	18.6	0.2	12	4.7	0.2	74.8	1.4
Farmville	H4	8	17.9	0.5	12	4.5	0.2	65.1	3.6
Forest Vale	H4	7	18.3	0.3	12	4.6	0.2	70.9	5.6
Kesen	H4	20	17.3	0.2	12	4.6	0.3	70.0	2.8
Menow	H4	6	18.9	0.2	12	4.5	0.3	71.0	6.3
Sylacauga	H4	10	19.4	0.3	12	4.7	0.3	71.9	2.2
Allegan	H5	20	17.8	0.4	12	4.6	0.3	72.0	2.3
Anlong	H5	20	19.2	0.6	12	4.7	0.3	71.0	2.0
Beardsley	H5	10	18.5	0.1	12	4.6	0.3	74.8	0.9
Changde	H5	20	19.8	0.9	12	5.0	0.2	69.0	2.0
Changxing*	H5	20	18.3	0.3	12	4.6	0.3	67.0	3.4
Enshi	H5	20	18.0	0.8	35	4.5	0.2	69.0	5.4
Jilin	H5	20	19.4	0.4	12	4.7	0.3	65.4	2.1
Limerick	H5	10	18.0	0.2	12	4.7	0.2	67.5	3.0
Mianchi	H5	20	19.6	0.4	10	4.8	0.5	63.0	6.1
Richardton	H5	8	17.7	0.2	16	4.5	0.2	68.7	4.8
Schenectady	H5	10	18.5	0.2	12	5.0	0.2	67.1	1.3
Tianzhang	H5	10	18.4	0.2	13	4.4	0.3	70.4	1.9
Zaoyang	H5	34	18.3	0.4	12	4.7	0.2	68.9	3.3
Butsura	H6	8	19.5	0.3	12	4.6	0.3	69.9	1.8
Guareña	H6	6	19.7	0.2	12	5.0	0.3	65.5	2.1
Lunan	H6	20	19.2	0.3	12	4.5	0.3	67.1	3.2
Mount Browne	H6	6	18.2	0.3	12	4.6	0.2	68.5	1.6
Nantong	H6	19	19.1	0.4	12	4.8	0.3	67.9	2.7
Ogi	H6	6	20.2	1.0	10	4.9	0.3	69.6	2.4
Wuan	H6	10	19.0	0.3	12	4.8	0.2	71.5	3.8
Xingyang	H6	20	20.2	0.4	12	4.9	0.3	68.3	8.1
Zhovtnevyi	H6	19	19.6	0.2	17	5.1	0.3	69.8	3.4
Bremervörde	H/L3.9	12	18.6	0.5	6	4.5	0.2	64.0	7.2
Tieschitz	H/L3.6				12	7.6	0.2	49.7	10.1
ALHA77011*	L3.5				9	8.0	0.8	51.6	10.9
Hedjaz	L3.7	8	24.2	0.4	8	7.3	0.5	55.8	8.2
Julesburg*	L3.7	8	22.8	0.6	9	6.7	0.2	64.5	3.3
Khohar	L3.6				8	9.1	2.0	56.4	11.0
Atarra	L4	10	23.6	0.2	13	7.4	0.3	65.4	5.0
Bald Mountain	L4	10	23.2	0.2	12	7.3	0.8	63.6	7.2
Barratta*	L4	8	23.4	0.4	12	7.0	0.4	67.4	3.8
pseudo-Bielokrynitschie	L4	10	24.3	0.2	5	7.9	0.4	73.9	2.6
Dalgety Downs*	L4	10	25.0	0.2	12	8.6	0.3	67.9	10.2
Hökmark	L4	10	23.9	0.2	12	7.8	0.4	63.5	10.3
Nikolskoe	L4	6	25.1	0.2	12	8.8	0.8	63.9	8.0
Rupota	L4	10	24.6	0.4	11	7.8	0.6	65.4	12.2
Saratov	L4	8	24.0	0.5	12	7.4	0.3	68.2	4.4
Slobodka	L4	10	23.6	0.4	13	7.5	0.4	62.9	6.7
Tennasilm	L4	8	23.0	0.1	12	7.2	0.4	61.3	10.4
Zhaodong	L4	37	24.4	0.4	6	8.4	0.4	53.8	2.1
Borkut	L5	10	24.9	0.2	11	8.0	0.4	73.8	1.0
Elenovka	L5	6	25.4	0.3	12	8.9	0.6	64.0	11.5
Fukutomi	L5	10	24.0	0.5	12	7.0	0.3	56.0	8.4
Homestead	L5	10	23.3	0.3	12	7.3	0.3	70.1	3.6
Innisfree	L5	9	25.3	0.2	15	7.8	1.1	56.5	6.2
Lishui	L5	20	25.7	0.3	10	8.2	0.4	70.8	1.8
Monte Milone	L5	10	25.0	0.3	11	8.3	0.2	63.7	8.0

Table 1. (Continued)

meteorite	type	Fa (mol%) n	Fa mean	Fa σ	Co (mg/g) n	Co mean	Co σ	Ni (mg/g) mean	Ni σ
Shelburne	L5	10	24.0	0.3	12	7.5	0.4	68.7	3.9
Alfianello	L6	20	25.0	0.5	10	8.6	1.1	60.1	5.3
Artracoona*	L6	10	25.5	0.2					
Barwell	L6	20	25.1	0.4	10	8.2	0.8	65.3	6.7
Bruderheim	L6	10	24.6	0.6	12	8.2	0.6	61.6	5.1
Denver	L6	8	25.4	0.2	13	7.5	2.0	63.8	9.5
Guangnan	L6	23	24.9	0.4	9	8.6	0.5	65.0	5.3
Guangrao	L6	20	25.3	0.4	10	7.8	0.9	60.8	9.5
La Criolla	L6	10	25.4	0.4	14	8.5	0.5	62.1	10.2
Lanxi	L6	8	25.0	0.2	10	7.5	0.6	63.3	8.3
Leedey	L6	20	25.4	0.3	10	8.1	1.0	66.0	4.8
Naiman	L6	8	25.1	0.3	10	9.5	0.5	62.2	6.8
Nan Yang Pao	L6	41	24.6	0.2	10	8.0	0.4	66.2	5.8
Peace River	L6	10	25.3	0.4	10	7.6	1.4	64.6	5.4
Peetz*	L6	10	25.7	0.2	12	8.1	0.6	75.4	0.8
Pierceville*	L6	10	25.8	0.4					
Salem	L6	10	24.2	0.2	12	8.4	0.4	66.2	5.1
Suizhou	L6	26	24.6	0.3	10	8.6	0.4	68.5	3.2
Tathlith	L6	10	25.8	0.3	5	8.8	0.4	74.6	1.3
Wethersfield (1971)	L6	12	25.0	0.3	12	8.1	1.2	70.8	4.4
Wethersfield (1982)	L6	12	25.3	0.3	17	8.5	1.1	68.3	3.9
Zavid	L6	10	24.1	0.3	12	7.8	1.1	64.0	5.9
Inman*	L/LL3.4				6	14.6	14.3	47.6	6.0
Bjurböle	L/LL4	8	26.2	0.2	12	12.6	2.0	63.0	7.6
Cynthiana	L/LL4	6	26.5	0.4	9	10.9	1.4	58.2	5.8
Vera*	L/LL4	10	25.7	0.4	12	9.8	0.7	66.6	12.5
Knyahinya	L/LL5	20	25.5	0.5	13	10.6	1.7	70.8	5.2
Qidong	L/LL5	126	25.7	0.5	8	15.8	1.5	68.0	2.0
Holbrook	L/LL6	10	25.7	0.3	12	10.4	0.6	72.4	4.1
Sultanpur	L/LL6	9	26.4	0.1	5	9.4	0.4	74.3	1.5
Trysil	L/LL6	10	26.3	0.2	11	9.0	0.3	72.3	3.7
Xi Ujimgin	L/LL6	20	26.4	0.2	3	8.0	0.7	75.9	1.2
ALHA77278*	LL3.6				9	65.0	79.3	64.6	16.8
ALH84086*	LL3.8	12	27.7	0.2	12	16.2	1.0	67.0	6.3
Bishunpur	LL3.1				8	5.3	1.1	37.7	6.5
Chainpur	LL3.4				13	11.2	1.1	49.3	6.2
Krymka	LL3.1				8	15.5	0.8	46.8	9.8
Manych	LL3.4				12	11.7	1.1	53.2	11.2
Ngawi	LL3.6				2	330	4.9	13.0	8.2
Parnallee	LL3.6				12	10.1	0.3	60.9	7.6
Semarkona	LL3.0				9	3.8	1.8	48.5	16.0
Albareto	LL4	5	26.6	0.2	10	14.4	0.7	56.3	8.7
EET87544*	LL4	9	32.4	0.2	1	302		40.0	
Bo Xian	LL4	12	28.6	0.6	12	14.2	2.9	49.0	7.6
Hamlet	LL4	10	26.9	0.9	10	15.8	2.0	63.0	14.8
Savtschenskoje	LL4	8	28.5	0.2	10	28.9	3.5	72.1	3.8
Soko-Banja	LL4	10	28.2	0.4	12	21.3	2.4	49.6	12.4
Alta'ameem	LL5	6	29.7	0.4	10	26.8	4.0	52.8	8.9
Guidder	LL5	8	28.9	0.1	7	30.2	3.8	49.7	8.9
Khanpur	LL5	10	28.2	0.3	10	37.9	1.1	53.2	8.7
Krähenberg	LL5	10	28.9	0.4	12	17.8	3.1	45.0	12.2
Nyirábrany	LL5	10	29.8	0.4	10	23.7	2.4	52.0	13.2
Olivenza	LL5	8	30.5	0.3	10	48.1	2.3	50.2	9.5
Parambu	LL5	12	32.0	0.5	1	370		16.0	
Richmond	LL5	10	27.9	0.3	9	14.7	0.6	47.7	4.9
Siena	LL5	9	29.0	0.4	12	27.4	3.4	47.5	6.5
Tuxtuac	LL5	10	30.3	0.2	10	58.7	4.9	66.9	2.0
ALH87906*	LL6	10	29.5	0.2	10	21.1	1.1	33.1	10.7
Appley Bridge	LL6	10	31.4	0.4	1	370		14.0	
Athens	LL6	8	30.7	0.3	1	30.8		68.4	
Dhurmsala	LL6	10	27.8	0.2	5	20.9	0.9	63.5	5.7
Dongtai	LL6	10	26.7	0.3	10	17.6	1.0	68.7	4.8
Ensisheim	LL6	10	29.0	0.7	12	22.2	1.7	56.5	2.7
Jelica	LL6	10	32.4	0.3	1	300		48.9	

Table 1. (Continued)

		Fa (mol%)			Co (mg/g)			Ni (mg/g)	
meteorite	type	n	mean	σ	n	mean	σ	mean	σ
Manbhoom	LL6	14	31.3	0.4	3	200	9.5	25.0	3.0
Mangwendi	LL6	10	30.2	0.3	8	25.6	1.4	46.2	8.8
Rugao	LL6	10	27.6	0.3	5	18.2	1.6	58.9	8.4
Saint Séverin	LL6	10	30.3	0.6	12	26.7	1.0	50.4	4.2
Uden	LL6	10	29.5	0.4	1	63.1		48.1	

*meteorite find.
Aberrant grains are excluded from the means and standard deviations.

mg/g Co) that are probably not kamacite (see below); their exclusion narrows the low-Ni metal (kamacite) range to 14.2–65.0 mg/g Co.

The ranges of the Ni content of H and L kamacite (57.5–74.8 and 51.6–75.4 mg/g Ni, respectively) are narrower than that of LL kamacite (33.1–72.1 mg/g Ni; excluding metal grains with ≥200 mg/g Co). It is possible that some of the metal grains with ≥70 mg/g Ni in L and LL chondrites are martensite, but the grains with <73 mg/g Ni do not exhibit a martensitic structure when etched with nital.

On the basis of the data in Table 1, group compositional ranges of olivine Fa and kamacite Co and Ni in equilibrated OCs can be rigorously determined (Table 3). [Aberrent grains (see below) were excluded from the ranges, means and standard deviations in Tables 1 and 3.] The mean group Fa and Co values increase from H to L to LL. Kamacite Ni ranges overlap considerably among the OCs; chondrites containing kamacite with >70 mg/g Ni occur in all three groups. Nevertheless, the lower extremes of the kamacite Ni ranges decrease from H to L to LL; the same is true for the group mean values. Because of the considerable overlap in group kamacite Ni ranges, olivine Fa and kamacite Co are much more useful than kamacite Ni for classification purposes.

Because olivine Fa and kamacite Co values are excellent classificatory parameters, KALLEMEYN et al. (1989) constructed a plot of kamacite Co (on a logarithmic scale) vs. olivine Fa (on a linear scale). An up-dated version of this diagram containing 113 meteorites from the present study appears in Fig. 1. The OCs plot on this diagram as an exponential function. The H group forms a tight cluster (except for two H3 chondrites) that is well-separated from the L and LL groups; the L cluster is not well-separated from those chondrites designated L/LL (see below); and the LL group plots as two poorly defined clusters at the right. One LL cluster consists of meteorites with kamacite containing ≤65 mg/g Co, the other of highly oxidized meteorites with metal containing ≥200 mg/g Co. (The Co-rich metal phase in the highly oxidized LL chondrites is probably not kamacite.) It seems likely that the apparent separation of the LL group into two clusters is an artifact caused by insufficiently representative sampling of the LL suite in the present study. (High-Fa LL chondrites are over-represented.)

There is no clear hiatus in olivine Fa and kamacite Co between the L and LL groups (Fig. 1). Following KALLEMEYN et al. (1989), I arbitrarily define the upper L boundary to be at the upper edge of the main L cluster (i.e., at Fa 25.8 mol% and kamacite Co 9.5 mg/g). (Incidentally, this definition excludes from the L group most chondrites with U, Th-He ages ≥ 3.2 Ga; J. T. WASSON, pers. comm.) Nine chondrites have mean Fa and/or Co values that lie between the L and LL ranges (Table 4). Five of these meteorites (Bjurböle, Cynthiana, Knyahinya, Qidong, and Xi Ujimgin) were analyzed by INAA (KALLEMEYN et al., 1989); their abundances of siderophile elements tend to be intermediate between L and

Table 2. Mean values of olivine Fa and martensite* Co and Ni for three shocked ordinary chondrites in which kamacite is absent.

meteorite	type+	Fa (mol%)	Co (mg/g)	Ni (mg/g)
Rose City	H5f	18.8	4.4	97.9
Jartai	L6e	25.1	5.7	160
Paragould	LL5d	28.1	18.9	89.1

*Metal grains with ≥77.0 mg/g Ni are considered to be martensite.

+Type includes shock facies determined by using the criteria of Dodd and Jarosewich (1979).

Table 3. Olivine Fa, kamacite Co and Ni compositional ranges for equilibrated ordinary chondrites.

	Fa (mol%) range	Fa (mol%) mean	Co (mg/g) range	Co (mg/g) mean	Ni (mg/g) range	Ni (mg/g) mean
H4-6	17.3-20.2	18.8	4.4-5.1	4.7	63.0-74.8	69.2
L4-6	23.0-25.8	24.7	7.0-9.5	8.0	53.8-75.4	65.4
LL4-6	26.6-32.4	29.4	14.2-370	77.4	14.0-72.1	49.8

The low-Ni, high-Co phase is included among the LL kamacite data. Aberrant grains are excluded from the ranges and means.

LL chondrites. Because these meteorites cannot be assigned unambiguously to either the L or LL group, they are designated here as L/LL chondrites. It is not clear, however, if these meteorites actually constitute a distinct chondrite group.

Qidong has the most divergent Fa and Co values of the L/LL chondrites. Its olivine Fa composition lies near the upper extreme of the L range and its kamacite Co content lies near the lower extreme of the LL range. WANG and RUBIN (1987) found that Qidong is intermediate between L and LL chondrites in many of its properties including modal abundance of metallic Fe-Ni and bulk O-isotopic composition (R. N. CLAYTON and T. K. MAYEDA, unpub. data, quoted in WANG and RUBIN, 1987).

The olivine compositional distribution of Inman (n = 135) (Fig. 5 of KEIL et al., 1978) has a large peak at Fa 25–27, spanning the hiatus between the L and LL Fa ranges (Table 3). The mean kamacite Co content of Inman (14.6 mg/g) is near the lower extreme of the LL range, but the large standard deviation (14.3 mg/g) makes this value highly uncertain. The bulk composition of Inman was determined by wet chemical techniques (Table 6 of KEIL et al., 1978), but the presence of Fe^{3+} in the sample poses difficulties in the assignment of iron to FeO, Fe_2O_3, and Fe metal. KEIL et al. (1978) classified Inman as an L3 chondrite, but HUSS (1987) subsequently classified it as an LL3 chondrite. Because Inman cannot be assigned unambiguously to either the L or LL chondrite groups, I tentatively include it with the nine other L/LL chondrites.

The INAA data of KALLEMEYN et al. (1989) show that two chondrites, Bremervörde and Tieschitz, are intermediate between H and L chondrites in their abundances of siderophile elements. Bremervörde has olivine Fa, kamacite Co, and kamacite Ni values within the H chondrite range; Tieschitz (which is too unequilibrated to have a meaningful mean Fa value) has kamacite Co in the L range and kamacite Ni in the LL range. The bulk O-isotopic compositions of these meteorites (R. N. CLAYTON, pers. comm.) do not resolve the ambiguities of their classification. On the standard three-isotope diagram, Tieschitz lies to the right of the LL4–6 range and in the vicinity of LL3 Chainpur, whereas Bremervörde lies within the L4–6 range. In light of these ambiguities, it seems prudent to accept the H/L classification for both of these meteorites (KALLEMEYN et al., 1989).

The olivine and kamacite compositional ranges (Table 3) serve to show that several chondrites from this study have been previously misclassified. Although GRAHAM et al. (1985) listed Innisfree as LL5, the Fa and Co values of this meteorite (Table 1) place it clearly within the L group. On this basis, Innisfree was reclassified as L5 (KALLEMEYN et al., 1989). Instrumental neutron activation analysis (INAA) of Innisfree confirms its new classification as an L chondrite (KALLEMEYN et al., 1989). Richmond was listed by GRAHAM et al. (1985) as L5, but its Fa and Co values place it in the LL group; I therefore reclassify Richmond as an LL5 chondrite. GRAHAM et al. (1985) listed Albareto as L4; however, its Fa value lies at the lower extreme of the LL range and its Co value lies within the LL range. If Albareto were excluded from the LL group, the lower extreme of the LL Fa range would increase only slightly, from 26.6 to 26.7 mol%; the kamacite Co range would not change at all. These considerations indicate that Albareto is best classified as an LL4 chondrite.

Bielokrynitschie is listed as an H4 chondrite (GRAHAM et al., 1985); G. KURAT (pers. comm.) confirmed this classification through his analyses of olivine and pyroxene in the main mass of Bielokrynitschie in the Naturhistorisches Museum in Vienna. My analyses of the Smithsonian Institution specimen of Bielokrynitschie show that this specimen is an L4 chondrite. This discrepancy probably reflects a sample mix-up and I hereafter refer to the Smithsonian specimen as pseudo-Bielokrynitschie.

It is worthwhile to examine portions of Fig. 1 at higher resolution (Fig. 2a,b,c). In these diagrams different petrologic types are designated by different symbols. In Fig. 2a (the H region), H3 and H4 chondrites tend to plot at the lower left, indicative of their low mean Fa and Co values; H5 chondrites are distributed uniformly throughout the main H field; and H6 chondrites tend to plot at the upper right, indicative of their high mean Fa and Co values.

A similar trend is evident in the L chondrite field (Fig. 2b). Julesburg (one of the two L3 chondrites plotted) lies at the extreme lower left, underscoring its low values of Fa and Co; L4 chondrites tend to plot toward the lower left; L5 chondrites are uniformly distributed throughout the L field; and L6 chondrites tend to plot at the upper right, indicative of their high Fa and Co values.

The LL chondrite field (Fig. 2c) shows very similar trends. LL3 and LL4 chondrites tend to plot at the lower left, LL5 chondrites tend to plot in the center, and LL6 chondrites tend to plot at the upper right. (ALH84086 (LL3.8), analyzed in the present study, is one of only two known LL3 chondrites

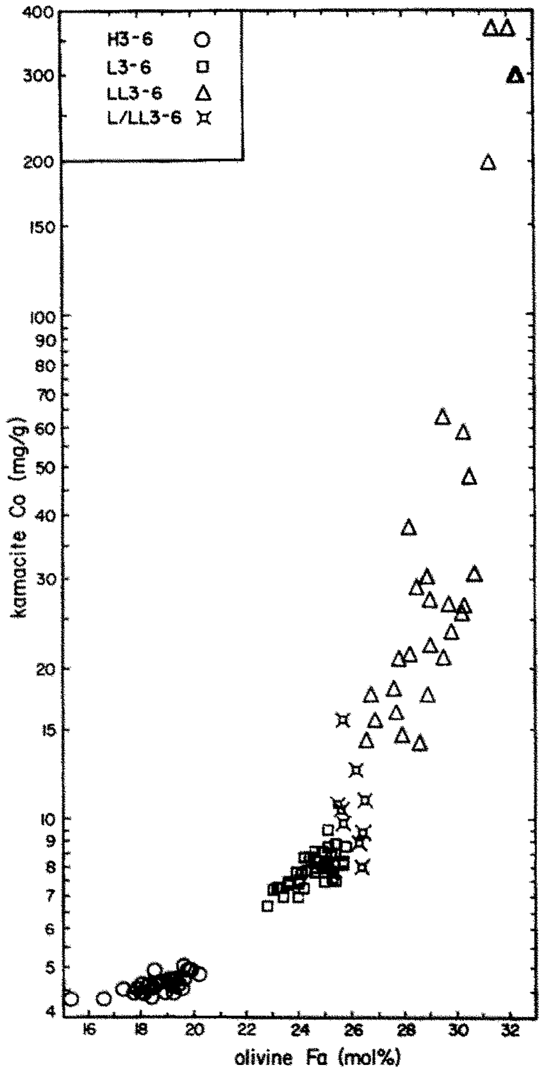

FIG. 1. Kamacite Co concentration vs olivine fayalite (Fa) content for 113 type 3–6 ordinary chondrites. Excluded from the plot are 14 type ≤3.6 chondrites (for which meaningful mean Fa values cannot be obtained), three severely shocked chondrites (which contain martensite but no kamacite), three severely weathered chondrites (in which all of the metal has been oxidized) and Netschaevo chondritic clasts (which plot off the lower left side of the diagram). The diagram shows the exponential relationship between kamacite Co and olivine Fa. H chondrites form a tight cluster at the lower left (except for two H3 chondrites which plot to the left of the main cluster); L chondrites form a tight cluster at the center; and LL chondrites span a large range at the right. There is no clear hiatus between the L and LL chondrites; the interval between them is occupied by ambiguously classified meteorites designated here as L/LL chondrites.

that are sufficiently equilibrated to yield meaningful mean Fa values; the other is Y-74191 (LL3.7); D. W. G. SEARS, pers. comm.)

These diagrams demonstrate that among OCs, the type-3 and type-4 members of each group tend to have lower olivine Fa and kamacite Co values than the type-5 and type-6 members (Table 5). These results confirm those of SCOTT et al. (1986) who found that mean FeO contents of olivine and low-Ca pyroxene increase by 3 to 5% in the OCs from type-4 to type-6. Also evident in Table 5 is that H3, L3, and LL3 chondrites have lower kamacite Ni contents than H6, L6, and LL6 chondrites, respectively. (The most glaring exception to this trend is ALH87906 (LL6) which has kamacite with less Ni (33.1 mg/g) than that in any other ordinary chondrite.)

With rare exceptions, olivine and kamacite are more heterogeneous in the type-3 and/or type-4 members of each OC group than the type-6 members (Table 5) (e.g., DODD et al., 1967; SEARS et al., 1980). Such a tendency is implicit in the definitions of the petrologic types (VAN SCHMUS and WOOD, 1967).

As shown in Table 3, the mean kamacite Ni content of equilibrated OCs decreases from H to L to LL. This trend is clearly shown in a histogram of the kamacite Ni distribution (Fig. 3). Although some meteorites within each group have kamacite grains with mean Ni contents above 70 mg/g, the proportions are not evenly distributed: 37% of H chondrites, 16% of L chondrites, and 3% of LL chondrites have kamacites with ≥70 mg/g Ni. With two (unplotted) exceptions (Tieschitz and Inman), the only chondrites with mean kamacite Ni concentrations ≤50 mg/g are LL. The Co-rich metal grains in the highly oxidized LL chondrites have Ni concentrations that extend even lower [13.0–48.9 mg/g Ni (Table 1)].

Intragroup olivine compositional distributions

Figure 2 clearly demonstrates that different meteorites of the same group and petrologic type can have significantly different mean olivine Fa and kamacite Co values. A careful examination of the means and standard deviations in Table 1 show that the compositional distributions of olivine in some meteorites of a particular group/type classification do not even overlap those of other meteorites of the same classification. For example, every analyzed olivine grain in H5 Mianchi (Fa 19.6 ± 0.4) is more ferroan than any analyzed grain in H5 Allegan (Fa 17.8 ± 0.4) as shown in Fig. 7.7.2 of RUBIN et al. (1988). There are many examples of this phenomenon in all three OC groups (e.g., H4 Kesen and H4 Sylacauga; L5 Homestead and L5 Lishui; and LL6 Dongtai and LL6 Jelica).

Table 4. Assignment of chondrite group on the basis of olivine Fa and kamacite Co for L/LL chondrites.

chondrite	type	Fa	Co
Bjurböle	4	L/LL	L/LL
Cynthiana	4	L/LL	L/LL
Holbrook	6	L	L/LL
Inman	3.4	L/LL	LL
Knyahinya	5	L	L/LL
Qidong	5	L	LL
Sultanpur	6	L/LL	L
Trysil	6	L/LL	L
Vera	4	L	L/LL
Xi Ujimgin	6	L/LL	L

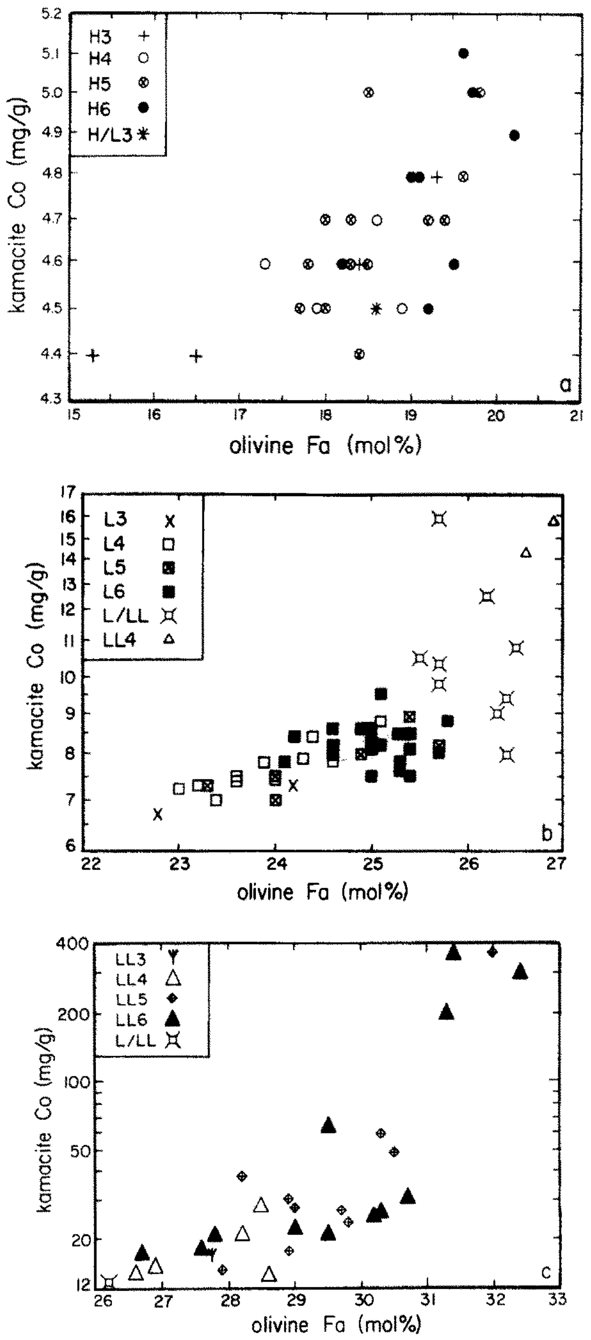

FIG. 2. Selected portions of the kamacite Co vs olivine Fa diagram shown in Fig. 1. Different petrologic types are denoted by distinct symbols. (a) The H region. H6 chondrites tend to have higher Fa and Co values than H3 and H4 chondrites. (b) The L and L/LL region. L6 chondrites tend to have higher Fa and Co values than L3 and L4 chondrites. (c) The LL region. LL6 chondrites tend to have higher Fa and Co values than LL3 and LL4 chondrites. Figure 2a, b, and c are not to the same scale.

Netschaevo

The Netschaevo iron meteorite contains chondrule-bearing silicate clasts (BREZINA, 1885; ZAVARITSKII and KVASHA, 1952; OLSEN and JAROSEWICH, 1971) that have been recrystallized to petrologic type-6 (BILD and WASSON, 1977). I have identified the following chondrule textural types in these clasts: barred olivine, porphyritic olivine, porphyritic pyroxene, porphyritic olivine-pyroxene, and radial pyroxene. The chondrules range in apparent diameter from 300 μm (1.74 ϕ) to 1200 μm (-0.26 ϕ) and average (n = 19) 720^{+360}_{-240} μm (0.48 $\pm$ 0.59 ϕ). (ϕ-units are defined by the relationship $\phi = -\log_2 d$, where d is the average apparent diameter of the chondrule in millimeters.) Because many small chondrules in Netschaevo may have been rendered unrecognizable during recrystallization, the given chondrule size range must be regarded as an upper limit. The chondritic clasts contain olivine, low-Ca pyroxene, Ca-rich pyroxene, plagioclase, merrillite, chlorapatite, chromite, troilite, schreibersite, and abundant metallic Fe-Ni (OLSEN and JAROSEWICH, 1971). My observations of slight to moderate undulose extinction in the olivine indicate that the clasts are of shock facies b, based on the criteria of DODD and JAROSEWICH (1979). Olivine (Fa 14.3 $\pm$ 0.3; n = 10) and low-Ca pyroxene (Fs 14.0 $\pm$ 0.2; n = 10) values are much lower than those in equilibrated H-L-LL chondrites (Table 1; KEIL and FREDRIKSSON, 1964), but the kamacite Co concentration (4.5 mg/g) is within (but near the lower extreme of) the H chondrite range. Thus, Netschaevo lies along the extrapolation of the Co-Fa curve in Fig. 1; this curve approaches the horizontal asymptotically at the lower left of the diagram.

The metallographic cooling rate of the chondritic clasts in Netschaevo was determined by measuring the sizes and central Ni contents of taenite grains (WOOD, 1967) and using the revised cooling rate curves of WILLIS and GOLDSTEIN (1981). Figure 4 indicates that the clasts cooled through 500°C (the temperature at which taenite compositional zoning developed) at a rate of ~3°C/Ma. This result is similar to the cooling rate of 1.4°C/Ma determined for the metal portions of Netschaevo by SCOTT and WASSON (1976) using the cooling-rate equation of WASSON (1971).

Aberrant grains

Equilibrated chondrites are characterized by sets of mineral grains with narrow compositional ranges (VAN SCHMUS and WOOD, 1967). For example, Table 1 shows that olivine in type 4–6 OCs has an average standard deviation of 0.3 mol% Fa; kamacite in type 4–6 H, L and LL chondrites has average standard deviations of 0.3, 0.6, and 2.2 mg/g Co, respectively (excluding high-Co grains in LL). In contrast to the homogeneity of most type 4–6 OCs, some (otherwise) equilibrated type 4–6 chondrites contain a few "aberrant" olivine and/or kamacite grains that are significantly out of equilibrium with the majority (e.g., SCOTT et al., 1985; Fig. 7.7.2 of RUBIN et al., 1988). SCOTT et al. (1985) estimated that aberrant mafic grains occur in at least 25%, and perhaps most, of the type 4–6 OCs.

Results from the present study show that kamacite grains differing in Co concentration by more than 3σ from the mean occur in 33% of type 4–6 OCs (Table 6). These aberrant kamacites are isolated grains located in the meteorite matrix; they are not sealed inside chondrules. Apparently aberrant kamacite grains were also found in three LL3 chondrites: Krymka, Manych, and Parnallee (Table 6); however, because

Table 5. Mean values and standard deviations of olivine Fa and kamacite Co and Ni for the different petrologic types of each OC group.*

	Fa (mol%)	σ_{Fa}	Co (mg/g)	σ_{Co}	Ni (mg/g)	σ_{Ni}
H3	17.6	1.6	4.6	0.2	66.7	4.8
H4	18.3	0.7	4.6	0.1	70.7	2.9
H5	18.6	0.7	4.7	0.2	68.8	3.0
H6	19.4	0.6	4.8	0.2	68.7	1.8
L3	23.5	1.0	7.8	1.0	57.1	5.4
L4	24.0	0.7	7.8	0.6	64.8	4.8
L5	24.7	0.8	7.9	0.6	65.5	6.6
L6	25.1	0.5	8.2	0.5	65.7	4.3
LL3	27.7	0.2	17.4	19.7	53.5	10.0
LL4	28.5	2.1	18.9	6.3	58.0	9.7
LL5	29.5	1.2	31.7	14.3	51.7	6.3
LL6	29.7	1.7	27.4	14.1	54.9	11.6

*The high-Co, low-Ni phase is excluded from the LL means.

these meteorites are unequilibrated, it is uncertain if these grains are truly aberrant.

WILLIS and GOLDSTEIN (1983) described isolated fine-grained plessite particles in an OC that they interpreted as untransformed bulk metal of the chondrite whole-rock. However, it seems plausible that these plessites are aberrant shock-produced martensite grains that unmixed during thermal metamorphism.

Aberrant-grain-bearing chondrites are considered to be fragmental breccias (e.g., SCOTT et al., 1985). The aberrant grains must have been incorporated into their hosts after the hosts cooled below high metamorphic temperatures; if the aberrant grains had been incorporated beforehand, their compositions would have equilibrated. Aberrant-grain-bearing fragmental breccias are analogous to those chondrites that contain impact-melt-clasts, exotic chondritic clasts or inclusions with anomalous O-isotopic compositions (e.g., RUBIN et al., 1983; EHLMANN et al., 1988; OLSEN et al., 1981).

The aberrant kamacite grains are not evenly distributed among the OC groups: 5 out of 29 H4–6 chondrites (17%), 17 out of 39 L4–6 chondrites (44%), and 8 out of 28 LL4–6 chondrites (29%) contain aberrant kamacites. As noted above, martensite is also most abundant in L chondrites and least abundant in H chondrites. These observations are consistent with the more pervasive collisional shock effects in L chondrites relative to H chondrites (e.g., ANDERS, 1964; HEYMANN, 1967; TAYLOR and HEYMANN, 1969, 1971; BOGARD et al., 1976). Similarly, RUBIN et al. (1983) found that impact-melt-rock- and/or exotic-clast-bearing fragmental breccias are appreciably more abundant among L (and LL) chondrites than among H chondrites.

Aberrant olivine grains were found in 21 of 96 type 4–6 OCs (22%), six of which also contain aberrant kamacite grains. Altogether, 47 of 105 type 4–6 OCs (i.e., roughly half) were

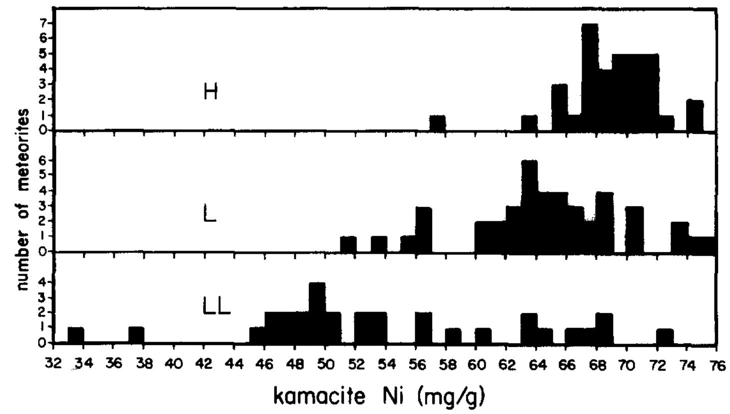

FIG. 3. Histogram of kamacite Ni concentration in H, L, and LL chondrites. Excluded from the diagram are those meteorites that contain the low-Ni, high-Co phase (with ≥200 mg/g Co). The kamacite Ni concentration is highest in H, intermediate in L, and lowest in LL chondrites.

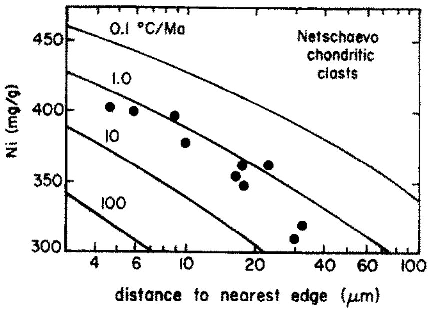

FIG. 4. Plot of the Ni content in the centers of taenite grains vs the distance to the nearest edge of the grains for a chondritic clast in the Netschaevo IIE-an iron. Cooling rate curves are from WILLIS and GOLDSTEIN (1981). The data plot coherently and indicate a metallographic cooling rate of ~3°C/Ma.

found to contain aberrant mafic and/or metal grains. Because only a limited number of grains were analyzed in each chondrite, it is highly probable that far more than half of the type 4–6 OCs are fragmental breccias.

Low-Ni, high-Co metal phase

Most OCs contain two predominant metallic Fe-Ni phases: kamacite and taenite. In addition, tetrataenite (ordered FeNi) has been identified in H, L, and LL chondrites of every petrologic type (CLARKE and SCOTT, 1980). Many shock-reheated OCs contain martensite, a phase typically containing 80–210 mg/g Ni, formed from high-temperature taenite during rapid cooling (e.g., TAYLOR and HEYMANN, 1971; SMITH and GOLDSTEIN, 1977). Awaruite (ideally Ni_3Fe) occurs in several LL3 chondrites (TAYLOR et al., 1981) and in LL5 Parambu (DANON et al., 1981; RUBIN, 1988) in association with troilite and pentlandite.

AFIATTALAB and WASSON (1980) first reported the occurrence of a new high-Co, low-Ni metal phase in an equilibrated clast in LL3 Ngawi. At about the same time, R. S. Clarke found an occurrence of this same phase in LL6 Appley Bridge (R. S. CLARKE, pers. commun.). The phase appears to have a maximum Co content of 370 mg/g and a maximum Ni content of 25 mg/g. In virtually every case the phase occurs at the interface between sulfide (troilite or pentlandite) and high-Ni metal (tetrataenite or awaruite) (Fig. 5). I have identified grains with 370 mg/g Co in Appley Bridge and Parambu and grains with 200–330 mg/g Co in EET87544, Jelica, Manbhoom, and Ngawi (Table 1). [In addition to these highly oxidized LL chondrites, metal grains with 370 mg/g Co occur in the highly oxidized ungrouped chondrite ALH85151 (RUBIN and KALLEMEYN, 1989)]. The phase typically occurs as ≤1–10 μm-size grains, although the one reported by AFIATTALAB and WASSON (1980) is 40 μm. Because X-ray analyses have not yet been done, the structure of this phase is unknown.

DISCUSSION

The continuous fractionation sequence and the formation of OC parent bodies

The three OC groups differ in their siderophile/lithophile element ratios; e.g., Ni/Mg varies from 0.114 in H chondrites to 0.081 in L chondrites to 0.067 in LL chondrites (WASSON and KALLEMEYN, 1988). These differences have been ascribed

Table 6. Mean and aberrant* kamacite Co contents (mg/g) in ordinary chondrites.

meteorite	type	mean	aberrant	meteorite	type	mean	aberrant
Farmville	H4	4.5±0.2	2.8	La Criolla	L6	8.5±0.5	11.0
Enshi	H5	4.5±0.2	3.7	Leedey	L6	8.1±1.0	4.0
Mianchi	H5	4.8±0.5	2.8	Naiman	L6	9.5±0.5	7.6
Schenectady	H5	5.0±0.2	3.2	Nan Yang Pao	L6	8.0±0.4	4.8
Tianzhang	H5	4.4±0.3	1.7	Wethersfield '82	L6	8.5±1.1	5.4
Mount Browne	H6	4.6±0.2	3.8	Trysil	L/LL6	9.0±0.3	13.7
Atarra	L4	7.4±0.3	5.0	Krymka	LL3	15.5±0.8	3.7
Bald Mountain	L4	7.3±0.8	10.3	Manych	LL3	11.7±1.1	3.6
Dalgety Downs	L4	8.6±0.3	13.1	Parnallee	LL3	10.1±0.3	15.6
Hökmark	L4	7.8±0.4	4.8	Albareto	LL4	14.4±0.7	19.2
Saratov	L4	7.4±0.3	6.0	Guidder	LL5	30.2±3.8	61.8
Slobodka	L4	7.5±0.4	9.7	Khanpur	LL5	37.9±1.1	28.4
Borkut	L5	8.0±0.4	6.2	Richmond	LL5	14.7±0.6	20.2
Homestead	L5	7.3±0.3	5.4	Tuxtuac	LL5	58.7±4.9	40.3
Lishui	L5	8.2±0.4	6.3	Dhurmsala	LL6	20.9±0.9	63.0
Shelburne	L5	7.5±0.4	5.9	Dongtai	LL6	17.6±1.0	106
Barwell	L6	8.2±0.8	4.2	Mangwendi	LL6	25.6±1.4	18.0
Bruderheim	L6	8.2±0.6	5.3				

*Aberrant grains are those that differ by >3σ from the mean. More than one aberrant grain was found in eight chondrites: Tianzhang, Dalgety Downs, Homestead, Barwell, Nan Yang Pao, Wethersfield (1982), Parnallee and Dhurmsala.

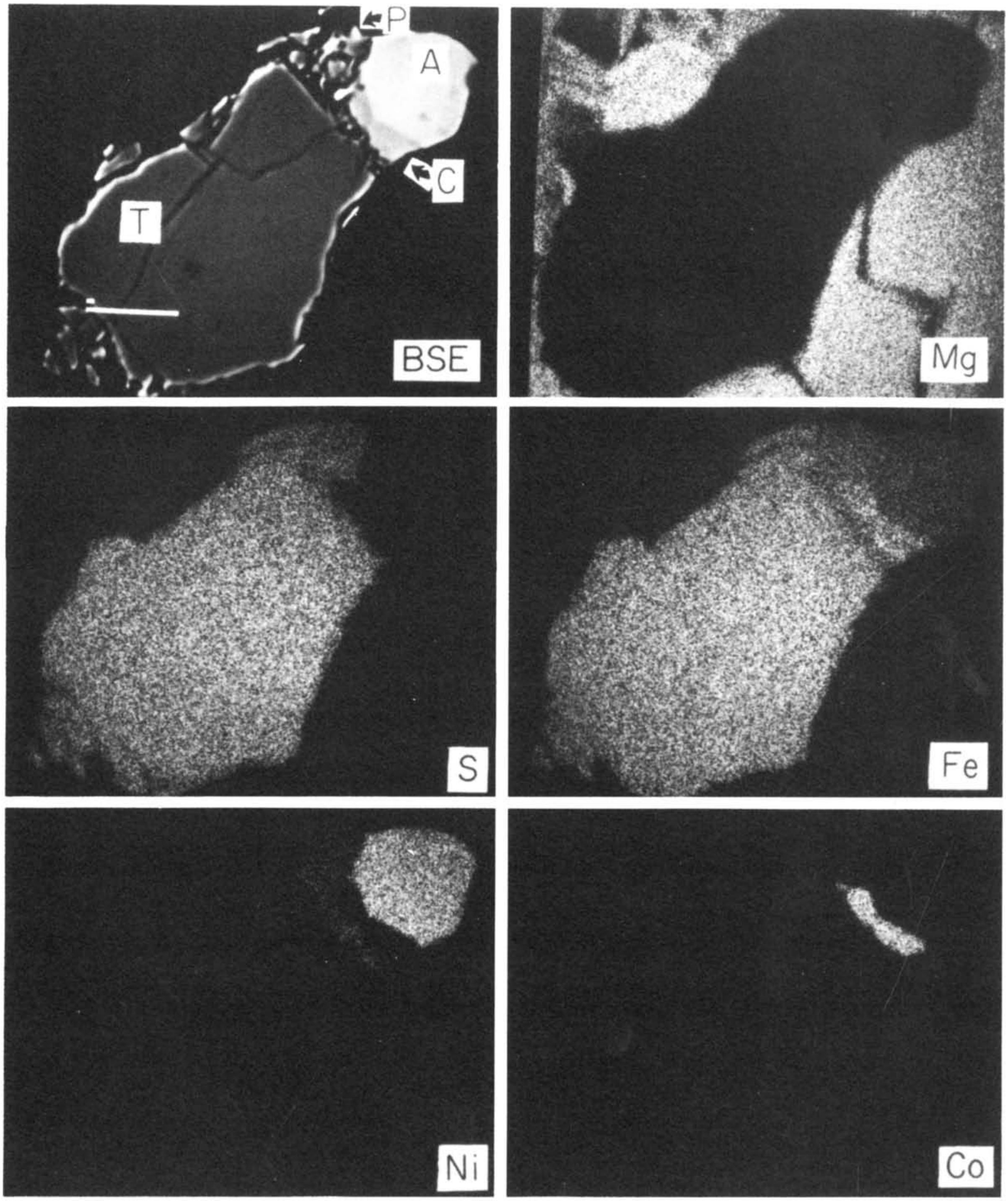

FIG. 5. Typical occurrence of the low-Ni, high-Co metallic Fe phase in the Parambu LL5 chondrite. The image at the upper left (BSE) was made with back-scattered electrons. The Co-rich phase (C) occurs at the interface between awaruite (A) and pentlandite (P). Adjacent to the pentlandite is troilite (T). The black areas surrounding the metal-sulfide assemblage are composed of olivine and pyroxene grains. The other five pictures are X-ray images of the indicated elements. The long white bar at the lower left of the BSE image is 10 μm in length; all six images are to the same scale.

to differing efficiencies in the agglomeration of metal and silicate particles during accretion (e.g., WASSON, 1985). TANDON and WASSON (1968) suggested that the oxidation state of OCs was related to the siderophile/lithophile (or metal/silicate) fractionation. MÜLLER et al. (1971) confirmed this suggestion and showed that OCs are related by a continuous fractionation sequence that varied smoothly with oxidation state. The zone of agglomeration of each individual chondrite group encompassed only a limited portion of the diverse nebular materials created by the continuous fractionation sequence (e.g., Figs. 3 and 4 of MÜLLER et al., 1971).

It seems likely that more than three OC parent bodies formed in the nebula, some with properties intermediate between H and L, and between L and LL, others with properties more extreme than H or LL. The paucity of meteorites with such compositions mainly reflects the fact that their parent bodies are not presently in efficient, meteorite-yielding orbits. Nevertheless, there may be samples from more than three OC groups in our collections; Tieschitz and Bremervörde (designated H/L) may come from a body intermediate in its properties between H and L chondrites; and at least some of the ten L/LL meteorites listed in Table 4 may come from a body intermediate between L and LL chondrites. It is very likely that Netschaevo comes from an OC body more extreme in its properties than H chondrites (BILD and WASSON, 1977; see below). Group IVA iron meteorites (whose oxygen isotopic composition is very similar to that of L chondrites; CLAYTON et al., 1983) may come from an OC parent body that melted and differentiated.

Classification of Netschaevo

The composition of the metal portions of the Netschaevo iron meteorite is similar to but slightly deviant from those of group-IIE irons (Fig. 1 of WASSON and WANG, 1986). Another anomalous property of Netschaevo is that it is the only iron meteorite with chondrule-bearing silicates (e.g., OLSEN and JAROSEWICH, 1971). The $\delta^{17}O$ and $\delta^{18}O$ values of these silicates are distinctly lower than those of the differentiated silicates in other IIE irons (e.g., Fig. 2 of WASSON and WANG, 1986). On the bases of these differences (particularly the O-isotope data), WASSON and WANG (1986) designated Netschaevo as IIE-an and concluded that it was probably derived from a different parent body than that of other IIE irons.

Several lines of evidence indicate that the chondritic silicates in Netschaevo belong to the OC clan: (1) their olivine Fa and kamacite Co values (14.3 mol% and 4.5 mg/g, respectively) lie along the extrapolation of the OC kamacite-olivine trend in Fig. 1; (2) their O-isotopic composition ($\delta^{17}O$ = 0.37‰, $\delta^{18}O$ = 3.53‰, relative to SMOW) lies along the OC slope-1 mixing line on the standard three-isotope diagram (Fig. 2 of WASSON and WANG, 1986); (3) on a diagram of reduced vs oxidized iron, Netschaevo silicates fall along an extension of the H-L-LL trend (BILD and WASSON, 1977); (4) siderophile element abundances are 60–100% greater in Netschaevo than in H chondrites (BILD and WASSON, 1977); and (5) most siderophile/Ni ratios are equivalent to those expected from H-L-LL trends (BILD and WASSON, 1977).

It can be concluded that Netschaevo is a member of a new OC group that is more reduced than H. BILD and WASSON (1977) were tempted to designate Netschaevo as an "HH chondrite," presumably standing for "very high total iron, very high metallic iron." Based on this suggestion and my petrographic studies of Netschaevo, I recommend that the silicates be classified as fragments of an HH6b ordinary chondrite.

Netschaevo probably formed by impact-melting of chondritic material, and separation and pooling of a metallic Fe-Ni liquid at the crater floor. The incorporation of unmelted chondritic "country rock" must have occurred rapidly, either through metallic liquid splattering or through foundering and sinking of chondritic debris into the metallic pool. Similar scenarios for the origin of group-IIE irons have been discussed by SCOTT and WASSON (1976), RUBIN et al. (1986), and WASSON and WANG (1986).

Intragroup differences in oxidation state

Chondrites sharing the same group/type classification (e.g., H5 Mianchi and H5 Allegan) that nevertheless have non-overlapping olivine compositional distributions occur in all three OC groups. Such chondrites as Mianchi and Allegan must have formed from material with significantly different oxidation states. This conclusion is supported by trace element data; Allegan (with a lower olivine Fa content) is appreciably richer in common siderophiles (Fe, Ni, Co) than Mianchi (Table 6 of KALLEMEYN et al., 1989).

These meteorites thus seem to represent materials that formed at slightly different times during the continuous fractionation sequence (or at slightly different nebular locations). Mianchi and Allegan may have been derived from (a) different H parent bodies or (b) from planetesimals that formed at opposite extremes of the H chondrite agglomeration zone. Because each asteroid has a unique collisional history, if case (a) were correct, there might be a correlation between olivine Fa and ^{21}Ne cosmic-ray exposure ages. Such data (compiled by KALLEMEYN et al., 1989) yield non-significant correlations ($r < 0.2$) for all three OC groups. This lack of correlation constitutes (non-definitive) evidence against Mianchi and Allegan coming from different parent bodies. It seems more likely that case (b) is correct and that these meteorites formed from widely separated regions of the H chondrite agglomeration zone, and that they eventually accreted into a single large H chondrite parent body. Analogous conclusions can be reached for members of the L and LL chondrite groups.

This scenario is consistent (but not exclusively so) with the model that chondrites with non-overlapping olivine compositional distributions were metamorphosed separately in small bodies prior to the accretion of large asteroids. As discussed by SCOTT and RAJAN (1981), it seems likely that maximum metamorphic temperatures were reached in small planetesimals that formed in different regions of the group's agglomeration zone. These planetesimals then cooled below their maximum temperatures prior to their assembly in a large parent body.

There are additional lines of evidence for the "metamorphosed-planetesimal" model of WASSON (1972) and SCOTT and RAJAN (1981): (a) the lack of correlation between metallographic cooling rate and petrologic type in each OC group (Fig. 5 of TAYLOR et al., 1987) indicates that by the time temperatures dipped below 500°C, OC parent bodies did not have layered "onion-shell" structures; (b) the occurrence in individual OC regolith breccias of different clasts that are of identical petrologic type but nevertheless possess significantly different metallographic cooling rates (e.g., Fig. 3 of WILLIAMS et al., 1985) indicates that different batches of chondritic material reached similar metamorphic temperatures at different burial depths. This, also, is inconsistent with an onion-shell model.

Intragroup differences in olivine Fa, kamacite Co, and kamacite Ni

As shown in Table 5, type-3 and type-4 chondrites in each OC group have lower olivine Fa and kamacite Co values than type-6 chondrites. Kamacite Ni values are lower in H3, L3, and LL3 chondrites than in H6, L6, and LL6 chondrites, respectively.

Lower FeO in the mafic silicates of type-3 chondrites may result either from (1) the lack of equilibration between fine FeO-rich silicates and coarse FeO-poor silicates in type-3 chondrites, or (2) initial bulk compositional differences between type-3 and type-6 chondrites. These models are discussed below:

1. Type-3 OCs contain 5–15 vol% fine-grained silicate matrix material containing very small (≤ 2 μm) grains of olivine with compositions of Fa 25–50 (HUSS et al., 1981). Because these tiny olivine grains are so difficult to analyze by electron microprobe, they are significantly under-represented in determinations of olivine compositional distributions. The mean Fa values of type-3 OCs are thus lower than they would otherwise be if these small FeO-rich grains were properly included. With increasing metamorphism, the tiny Fa-rich olivines from the matrix tend to equilibrate with larger isolated olivine grains and olivine chondrule phenocrysts that have lower FeO contents; the mean Fa contents of the olivine compositional distributions of type-4 to type-6 OCs are thus increased.
   The tendency for small Fa-rich olivines to equilibrate with coarser lower-Fa olivines during metamorphism could lead to size-dependent compositional differences in the olivine Fa contents of the transitional type-4 OCs. KALLEMEYN et al. (1989) investigated this possibility by analyzing large (≥ 80 μm) olivine grains (chondrule phenocrysts and isolated crystals) and small (5–10 μm) olivine grains (from the matrix) of four type-4 OCs (Albareto, Bjurböle, Saratov, and Tennasilm); no resolvable differences in composition were found. Thus, model 1 may not be an entirely adequate explanation of the lower olivine Fa contents of type-3 OCs.
2. SCOTT et al. (1986) suggested that the lower FeO contents of mafic silicates in type-3 chondrites reflect compositional differences of initial bulk between type-3 and type-6 chondrites. If this is the case, one can infer that type-3 (and type-4) chondrites formed with lower oxidation states than type-6 chondrites. It is possible that the type-3 and type-4 chondrites accreted fewer type-II (FeO-rich) chondrules or less FeO-rich fine-grained matrix material, possibly because the amount of these materials settling to the nebular midplane varied with time. Although the recrystallized nature of type-6 chondrites precludes petrographic testing of these possibilities, the abundances of type-II chondrules (or the type-I/type-II chondrule abundance ratio), at least, could be determined readily in type 3–5 chondrites.

Such a proposed correlation between the petrologic type of an OC and its abundance of type-II chondrules or fine-grained matrix material would be somewhat analogous to the situation in CO3 chondrites, where metamorphic grade is correlated with the abundance of amoeboid olivine inclusions as well as mean chondrule size (RUBIN, 1989; RUBIN et al., 1985).

The lower kamacite Co and Ni values in type-3 relative to type-6 OCs require a different explanation. In equilibrated chondrites, typified by type-6 OCs, Co resides primarily in kamacite and Ni resides primarily in taenite and tetrataenite. However, this is not the case in the primitive ungrouped chondrites Renazzo, Al Rais, and ALH85085, or in the complex breccia, Bencubbin. In these meteorites, Ni-rich metal contains more Co than kamacite (GROSSMAN et al., 1988; WEISBERG et al., 1988). In addition, the different metal phases in these meteorites have approximately cosmic Co/Ni ratios (e.g., Fig. 9 of GROSSMAN et al., 1988). It is probable that these meteorites contain a nebular metal component with positively correlated Ni and Co (GROSSMAN et al., 1988); this component may have formed by low-temperature oxidation of metal in the nebula.

Relicts of this component may also occur in the least-equilibrated type-3 chondrites; if so, one would predict that kamacite in these meteorites would contain low Co and low Ni, and that taenite or tetrataenite would contain high Co. This is consistent with (a) the unusually low kamacite Co values in LL3.0 Semarkona (3.8 mg/g) and LL3.1 Bishunpur (5.3 mg/g) compared to those of LL4-6 chondrites (≥ 14.2 mg/g) (Tables 1,3), (b) the low kamacite Ni value in Bishunpur (37.7 mg/g) compared to the LL4–6 average (excluding the high-Co phase) of 54.3 mg/g (kamacite in Semarkona has 48.5 mg/g Ni; Table 1), and (c) the occurrence of high-Co, high-Ni metal in several highly unequilibrated chondrites. Two such Co-rich tetrataenite grains (15.7 and 17.1 mg/g Co) occur in Semarkona (Fig. 5 of AFIATTALAB and WASSON, 1980); one grain with 13 mg/g Co occurs in Colony (one of the least-equilibrated CO3 chondrites; RUBIN et al., 1985); and one grain with 14 mg/g Co occurs in ALH85085 (Table 4 of GROSSMAN et al., 1988). [Although some equilibrated highly oxidized chondrites such as Appley Bridge and Parambu contain Ni-rich metal with up to 30 mg/g Co (A. E. RUBIN, unpubl. data), each of these chondrites also contains low-Ni metal that is much richer in Co].

There is an alternative mechanism that can account for low kamacite Co and Ni contents in the least equilibrated type-3 chondrites. Significant reduction of FeO to Fe metal may have taken place during chondrule formation (e.g., RAMBALDI et al., 1980; RAMBALDI and WASSON, 1982). Evidence for this is found in the common occurrence of tiny (≤ 2 μm-size), low-Ni (≤ 10 mg/g) metallic Fe inclusions within olivine phenocrysts of porphyritic chondrules in type-3 OCs (RAMBALDI and WASSON, 1982). Reduction of FeO to Fe would serve to dilute the Co and Ni concentrations of pre-existing metal while preserving the initial Co/Ni ratios. Because some of the analyzed metal grains in this study may have been derived from chondrules, it is possible that reduction during chondrule formation is responsible in part for the low kamacite Co and Ni values of type-3 OCs. Nevertheless, this mechanism cannot account for the occurrence of Co-rich tetrataenite grains in Semarkona, Colony, and ALH85085. A nebular metal component with correlated Ni and Co is still required.

Compositional variation of olivine with kamacite

In the kamacite Co-olivine Fa diagram (Fig. 1), it is apparent that LL chondrites have a much larger range in kamacite Co than either H or L chondrites. The Co-Fa curve increases exponentially from the H to the LL region; for example, in the L field, a 2 mol% increase in Fa corresponds to an increase of less than 3 mg/g Co (Fig. 2b), but in the middle of the LL field, a 2 mol% increase in Fa corresponds to an increase of more than 30 mg/g Co (Fig. 2c). This effect is due to the small amount of metallic Fe-Ni in LL chondrites, as low as ~14 mg/g in the highly oxidized LL chondrite, Parambu (DANON et al., 1981). For every metal particle that gets oxidized in an equilibrated LL chondrite, there are many olivine and pyroxene grains available to incorporate the liberated FeO; thus, for each modest increase in whole-rock oxidation state, there is only a modest increase in the mean FeO/(FeO + MgO) ratios of mafic grains. However, Co does not oxidize as readily as Fe; reduced Co liberated from oxidized metal is readily incorporated only into the remaining kamacite grains. Because such grains are rare, each one becomes significantly enriched in Co for each modest increase in whole-rock oxidation state (e.g., AFIATTALAB and WASSON, 1980). The net result is the exponential relationship between olivine Fa and kamacite Co shown in Fig. 1.

Variation of Co and Ni in OC kamacite

In going through the H-L-LL sequence, kamacite becomes systematically richer in Co and poorer in Ni (Table 3). I offer two possible alternative mechanisms to explain this trend (see below).

1. In the H-L-LL sequence of increasing degree of oxidation, Co replaces Ni in kamacite at low temperatures. This is the simplest explanation for the trend. However, it is in apparent conflict with the experiments of WIDGE and GOLDSTEIN (1977) which show that the addition of Co to the Fe-Ni-Co system causes kamacite to become richer in Co *and* Ni as temperatures decrease from 800° to 650°C. Although it cannot be ruled out that the effect reverses at low temperatures (≤400°C), I tentatively reject mechanism 1.
2. The presence of large (>200 μm) kamacite grains in many H chondrites and the paucity of such large grains in LL chondrites indicate that kamacite grain size decreases systematically through the H-L-LL sequence. Bulk H chondrite metal has less Ni than L or LL metal and during initial cooling enters the two-phase region of the Fe-Ni phase diagram at higher temperatures. If kamacite grain growth effectively ceases at the same low temperature in all three OC groups, it is apparent that H chondrite kamacite has a longer period of grain growth. This is consistent with the data of DODD (1976) who found that mean sizes of metal particles (including kamacite, taenite, and tetrataenite) are 540 μm in H3, 510 μm in L3, and 410 μm in LL3 chondrites. The difference in size between H and LL kamacite grains may be even larger. Smaller kamacite grains, preferentially occurring in LL chondrites, have their centers closer to their edges, thereby allowing diffusional processes to affect their centers more readily.

In the Fe-Ni phase diagram (Fig. 15 of REUTER et al., 1988), the kamacite solvus bends back on itself at temperatures below ~500°C and acquires a positive slope. Thus, kamacite can accommodate less Ni at lower temperatures than at higher temperatures. Small kamacite grains would tend to reach equilibrium faster than large grains and thus acquire less Ni. This effect is obvious in the metallographic cooling rate plots of WOOD (1967, Figs. 8, 9) which show that small kamacite grains contain less Ni than large grains. Thus, as kamacite grain size decreases through the H-L-LL sequence, equilibrium is more closely approached and the grains become poorer in Ni. (Because the amount of Ni taken up by kamacite is a function of cooling rate, this model assumes that there are no systematic differences in cooling rates among the OC groups).

The concomitant enrichment of Co in kamacite is a separate effect resulting from the increasing oxidation state of the OCs, the strong siderophilic character of Co, and its tendency to be accommodated into the kamacite crystal structure.

Formation of the low-Ni, high-Co metal phase

The presence of the low-Ni metal phase with 200–370 mg/g Co in the OCs appears to be restricted to those LL chondrites with mean Fa contents exceeding 31 mol% and to similarly oxidized portions of LL3 chondrite breccias (e.g., Ngawi). The equilibrated chondrites that possess this phase generally do not contain kamacite with <65 mg/g Co. The sole exception is Parambu, which is a light/dark fragmental breccia (DANON et al., 1981). Only one grain of kamacite (with 26.8 mg/g Co) was found in Parambu; this grain is probably aberrant.

It seems likely that the high-Co phase formed as a result of low-temperature processes. Metamorphic equilibration of highly oxidized LL chondrites above ~700°C resulted in taenite being the only metal phase present in these meteorites. After post-metamorphic cooling to low temperatures (≤325°C), Ni partitioned into tetrataenite or awaruite. Electron microprobe analyses of tetrataenite and awaruite in highly oxidized LL chondrites show that these phases apparently cannot accommodate ≥30 mg/g Co in the presence of the low-Ni, high-Co phase (A. E. RUBIN, unpubl. data). With decreasing temperatures, it seems likely that excess Co was liberated at the sulfide/Ni-rich-metal boundaries. The low-Ni, high-Co phase nucleated at these boundaries, perhaps by scavenging Fe from the Ni-rich metal.

It is not yet known if the low-Ni, high-Co phase has the body-centered cubic structure of kamacite. The phase is probably not wairauite (CoFe) which contains ~490 mg/g Co and most likely has the ordered CsCl structure (CHALLIS and LONG, 1964); analyses of the high-Co phase in the present study show that Co does not exceed 370 mg/g. Clarification of the structure of this phase requires additional work.

CONCLUSIONS

Early in solar system history, solid materials differentially settling to the nebular midplane resulted in a continuous fractionation sequence that established systematic compositional variations with heliocentric distance. Individual OC parent bodies acquired their particular compositions from the limited zone from which they agglomerated material. Each parent body probably formed by the accretion of planetesimals that already had cooled below their maximum metamorphic temperatures.

It seems likely that more than three OC parent bodies were originally formed; however, only the H, L, and LL bodies, or their collisional remnants, are now in efficient meteorite-yielding orbits. Netschaevo is from another OC parent body that is more reduced and richer in siderophiles than H chondrites. Tieschitz and Bremervörde may be from a body intermediate in its properties between H and L chondrites; analogously, Bjurböle, Cynthiana, Holbrook, Inman, Knyahinya, Qidong, Sultanpur, Trysil, Vera, and Xi Ujimgin may be from a parent body intermediate in its properties between L and LL chondrites. Group IVA irons may come from an OC parent body that melted and differentiated.

Even within a single OC parent body there is significant compositional variation. Different meteorites may represent material acquired at opposite extremes of the parent body's agglomeration zone. It is possible, but far from established, that variations of mineralogical composition with petrologic type reflect temporal changes in the proportion of material accreted to the parent body. The lower kamacite Co and Ni contents of type-3 OCs may reflect the presence of a relict nebular metal component with correlated Co and Ni; evidence for this component was obliterated in the higher petrologic types by metamorphic equilibration.

The occurrence of aberrant mafic and metal grains in at least half, and probably virtually all, of the OCs reflects the pervasiveness of asteroidal collisions after parent bodies had cooled below their maximum metamorphic temperatures. The different proportions of fragmental and regolith breccias among the three main OC groups (RUBIN et al., 1983) reflect the stochastic nature of collisional processes.

Acknowledgments—I thank J. T. Wasson, J. N. Grossman, and M. D. Barton for discussions; E. R. D. Scott, J. I. Goldstein, and G. J. Taylor for informal comments and their reviews of the manuscript; and R. E. Jones, R. Alkaly, and T. Jen for technical assistance. I am grateful to G. Kurat for his confirmation of the proper classification of Bielokrynitschie. Thin sections were generously provided by R. S. Clarke and T. B. Thomas of the Smithsonian Institution and by the Antarctic Meteorite Working Group. This work was supported in part by NASA Grant NAG 9-40.

Editorial handling: W. R. van Schmus

REFERENCES

AFIATTALAB F. and WASSON J. T. (1980) Composition of the metal phases in ordinary chondrites: Implications regarding classification and metamorphism. *Geochim. Cosmochim. Acta* **44**, 431–446.

ANDERS E. (1964) Origin, age, and composition of meteorites. *Space Sci. Rev.* **3**, 583–714.

BENCE A. E. and ALBEE A. L. (1968) Empirical correction factors for the electron microanalysis of silicates and oxides. *J. Geol.* **76**, 382–403.

BILD R. W. and WASSON J. T. (1977) Netschaevo: A new class of chondritic meteorite. *Science* **197**, 58–62.

BOGARD D. D., HUSAIN L., and WRIGHT R. J. (1976) ^{40}Ar-^{39}Ar dating of collisional events in chondrite parent bodies. *J. Geophys. Res.* **81**, 5664–5678.

BREZINA A. (1885) Die Meteoritensammlung des k.k. mineralogischen Hofkabinetes in Wien am 1. Mai 1885. *Jahrb. Geol. Reichsanst. Wien* **35**, 151–276.

CHALLIS G. A. and LONG J. V. P. (1964) Wairauite—a new cobalt-iron mineral. *Mineral. Mag.* **33**, 942–948.

CLARKE R. S. JR. and SCOTT E. R. D. (1980) Tetrataenite—ordered FeNi, a new mineral in meteorites. *Amer. Mineral.* **65**, 624–630.

CLAYTON R. N., MAYEDA T. K., OLSEN E. J., and PRINZ M. (1983) Oxygen isotope relationships in iron meteorites. *Earth Planet. Sci. Lett.* **65**, 229–232.

CRABB J. and SCHULTZ L. (1981) Cosmic ray exposure ages of the ordinary chondrites and their significance for parent body stratigraphy. *Geochim. Cosmochim. Acta* **45**, 2151–2160.

DANON J., CHRISTOPHE MICHEL-LÉVY M., JEHANNO C., KEIL K., GOMES C. B., SCORZELLI R. B., and SOUZA AZEVEDO I. (1981) Awaruite (Ni_3Fe) in the genomict LL chondrite Parambu: Formation under high fO_2 (abst.). *Meteoritics* **16**, 305.

DEER W. A., HOWIE R. A., and ZUSSMAN J. (1982) *Rock-forming Minerals, Vol. 1A, Orthosilicates,* 2nd edn. Longman House, London.

DODD R. T. (1976) Accretion of the ordinary chondrites. *Earth Planet. Sci. Lett.* **30**, 281–291.

DODD R. T. and JAROSEWICH E. (1979) Incipient melting in and shock classification of L-group chondrites. *Earth Planet. Sci. Lett.* **44**, 335–340.

DODD R. T., VAN SCHMUS W. R., and KOFFMAN D. M. (1967) A survey of the unequilibrated ordinary chondrites. *Geochim. Cosmochim. Acta* **31**, 921–951.

EHLMANN A. J., SCOTT E. R. D., KEIL K., MAYEDA T. K., CLAYTON R. N., WEBER H. W., and SCHULTZ L. (1988) Origin of fragmental and regolith meteorite breccias—Evidence from the Kendleton L chondrite breccia. *Proc. Lunar Planet. Sci. Conf. 18th,* 545–554.

FREDRIKSSON K., NELEN J., and FREDRIKSSON B. J. (1968) The LL-group chondrites. In *Origin and Distribution of the Elements* (ed. L. H. AHRENS), pp. 457–466. Pergamon Press.

FREER R. (1981) Diffusion in silicate minerals and glasses: A data digest and guide to the literature. *Contrib. Mineral. Petrol.* **76**, 440–454.

FRULAND R. M. (1975) Volatile movement in the Rose City meteorite, implications concerning the impact and late thermal history of ordinary chondrites (abstr.). *Meteoritics* **10**, 403–404.

GOMES C. B. and KEIL K. (1980) *Brazilian Stone Meteorites.* Univ. New Mexico Press.

GRAHAM A. L., BEVAN A. W. R., and HUTCHISON R. (1985) *Catalogue of Meteorites.* Univ. Arizona Press.

GROSSMAN J. N., RUBIN A. E., and MACPHERSON G. J. (1988) ALH85085: A unique volatile-poor carbonaceous chondrite with possible implications for nebular fractionation processes. *Earth Planet. Sci. Lett.* **91**, 33–54.

HEYMANN D. (1967) On the origin of hypersthene chondrites: Ages and shock effects of black chondrites. *Icarus* **6**, 189–221.

HUSS G. R. (1987) The role of presolar dust in the formation of the solar system. Ph.D. thesis, Univ. Minnesota, Minneapolis.

HUSS G. R., KEIL K., and TAYLOR G. J. (1981) The matrices of unequilibrated ordinary chondrites: Implications for the origin and history of chondrites. *Geochim. Cosmochim. Acta* **45**, 33–51.

KALLEMEYN G. W., RUBIN A. E., WANG D., and WASSON J. T.

(1989) Ordinary chondrites: Bulk compositions, classification, lithophile-element fractionations, and composition-petrographic type relationships. *Geochim. Cosmochim. Acta* **53**, 2747–2767.

KEIL K. and FREDRIKSSON K. (1964) The iron, magnesium, and calcium distribution in coexisting olivines and rhombic pyroxenes of chondrites. *J. Geophys. Res.* **69**, 3487–3515.

KEIL K., LUX G., BROOKINS D. G., KING E. A., KING T. V. V., and JAROSEWICH E. (1978) The Inman, McPherson County, Kansas meteorite. *Meteoritics* **13**, 11–22.

MASON B. and WIIK H. B. (1966) The composition of the Bath, Frankfort, Kakangari, Rose City, and Tadjera meteorites. *Amer. Mus. Novit.* **2272**, 1–24.

MÜLLER O., BAEDECKER P. A., and WASSON J. T. (1971) Relationship between siderophilic-element content and oxidation state of ordinary chondrites. *Geochim. Cosmochim. Acta* **35**, 1121–1137.

OLSEN E. J. and JAROSEWICH E. (1971) Chondrules: First occurrence in an iron meteorite. *Science* **174**, 583–585.

OLSEN E. J., MAYEDA T. K., and CLAYTON R. N. (1981) Cristobalite-pyroxene in an L6 chondrite: Implications for metamorphism. *Earth Planet. Sci. Lett.* **56**, 82–88.

PRIOR G. T. (1916) On the genetic relationship and classification of meteorites. *Mineral. Mag.* **18**, 28–44.

RAMBALDI E. R. and WASSON J. T. (1982) Fine, nickel-poor Fe-Ni grains in the olivine of unequilibrated ordinary chondrites. *Geochim. Cosmochim. Acta* **46**, 929–939.

RAMBALDI E. R., SEARS D. W., and WASSON J. T. (1980) Si-rich Fe-Ni grains in highly unequilibrated chondrites. *Nature* **287**, 817–820.

REUTER K. B., WILLIAMS D. B., and GOLDSTEIN J. I. (1988) Low temperature phase transformations in the metallic phases of iron and stony-iron meteorites. *Geochim. Cosmochim. Acta* **52**, 617–626.

RUBIN A. E. (1985) Impact melt products of chondritic material. *Rev. Geophys.* **23**, 277–300.

RUBIN A. E. (1988) Kamacite in ordinary chondrites (abstr.). *Meteoritics* **23**, 299.

RUBIN A. E. (1989) Size-frequency distributions of chondrules in CO3 chondrites. *Meteoritics* **24**, 179–189.

RUBIN A. E. and KALLEMEYN G. W. (1989) Carlisle Lakes and Allan Hills 85151: Members of a new chondrite grouplet. *Geochim. Cosmochim. Acta* **53**, 3035–3044.

RUBIN A. E., REHFELDT A., PETERSON E., KEIL K., and JAROSEWICH E. (1983) Fragmental breccias and the collisional evolution of ordinary chondrite parent bodies. *Meteoritics* **18**, 179–196.

RUBIN A. E., JAMES J. A., KECK B. D., WEEKS K. S., SEARS D. W. G., and JAROSEWICH E. (1985) The Colony meteorite and variations in CO3 chondrite properties. *Meteoritics* **20**, 175–196.

RUBIN A. E., JERDE E. A., ZONG P., WASSON J. T., WESTCOTT J. W., MAYEDA T. K., and CLAYTON R. N. (1986) Properties of the Guin ungrouped iron meteorite: The origin of Guin and of group-IIE irons. *Earth Planet. Sci. Lett.* **76**, 209–226.

RUBIN A. E., FEGLEY B., and BRETT R. (1988) Oxidation state in chondrites. In *Meteorites and the Early Solar System* (eds. J. F. KERRIDGE and M. S. MATTHEWS), pp. 488–511. Univ. Arizona Press.

VAN SCHMUS W. R. and WOOD J. A. (1967) A chemical-petrologic classification for the chondritic meteorites. *Geochim. Cosmochim. Acta* **31**, 747–765.

SCOTT E. R. D. and RAJAN R. S. (1981) Metallic minerals, thermal histories and parent bodies of some xenolithic, ordinary chondrite meteorites. *Geochim. Cosmochim. Acta* **45**, 53–67.

SCOTT E. R. D. and WASSON J. T. (1976) Chemical classification of iron meteorites—VIII. Groups IC, IIE, IIIF and 97 other irons. *Geochim. Cosmochim. Acta* **40**, 103–115.

SCOTT E. R. D., LUSBY D., and KEIL K. (1985) Ubiquitous brecciation after metamorphism in equilibrated ordinary chondrites. *Proc. Lunar Planet. Sci. Conf. 16th*, D137–D148.

SCOTT E. R. D., TAYLOR G. J., and KEIL K. (1986) Accretion, metamorphism, and brecciation of ordinary chondrites: Evidence from petrologic studies of meteorites from Roosevelt County, New Mexico. *Proc. Lunar Planet. Sci. Conf. 17th*, E115–E123.

SEARS D. W. and AXON H. J. (1976) Ni and Co content of chondritic metal. *Nature* **260**, 34–35.

SEARS D. W., GROSSMAN J. N., MELCHER C. L., ROSS L. M., and MILLS A. A. (1980) Measuring metamorphic history of unequilibrated ordinary chondrites. *Nature* **287**, 791–795.

SMITH B. A. and GOLDSTEIN J. I. (1977) The metallic microstructures and thermal histories of severely reheated chondrites. *Geochim. Cosmochim. Acta* **41**, 1061–1072.

STÖFFLER D., BISCHOFF A., BUCHWALD V., and RUBIN A. E. (1988) Shock effects in meteorites. In *Meteorites and the Early Solar System*, (eds. J. F. KERRIDGE and M. S. MATTHEWS), pp. 165–202. Univ. Arizona Press.

TANDON S. N. and WASSON J. T. (1968) Gallium, germanium, indium and iridium variations in a suite of L-group chondrites. *Geochim. Cosmochim. Acta* **32**, 1087–1109.

TAYLOR G. J. and HEYMANN D. (1969) Shock, reheating, and the gas retention ages of chondrites. *Earth Planet. Sci. Lett.* **7**, 151–161.

TAYLOR G. J. and HEYMANN D. (1971) Postshock thermal histories of reheated chondrites. *J. Geophys. Res.* **76**, 1879–1893.

TAYLOR G. J., OKADA A., SCOTT E. R. D., RUBIN A. E., HUSS G. R., and KEIL K. (1981) The occurrence and implications of carbide-magnetite assemblages in unequilibrated ordinary chondrites (abstr.). *Lunar Planet. Sci.* **12**, 1076–1078.

TAYLOR G. J., MAGGIORE P., SCOTT E. R. D., RUBIN A. E., and KEIL K. (1987) Original structures, and fragmentation and reassembly histories of asteroids: Evidence from meteorites. *Icarus* **69**, 1–13.

WANG D. and RUBIN A. E. (1987) Petrology of nine ordinary chondrite falls from China. *Meteoritics* **22**, 97–104.

WASSON J. T. (1971) An equation for the determination of iron-meteorite cooling rates. *Meteoritics* **6**, 139–147.

WASSON J. T. (1972) Formation of ordinary chondrites. *Rev. Geophys. Space Phys.* **10**, 711–759.

WASSON J. T. (1985) *Meteorites: Their Record of Early Solar System History.* W. H. Freeman.

WASSON J. T. and KALLEMEYN G. W. (1988) Compositions of chondrites. *Phil. Trans. Roy. Soc. Lond. A* **325**, 535–544.

WASSON J. T. and WANG J. (1986) A nonmagmatic origin of group-IIE iron meteorites. *Geochim. Cosmochim. Acta* **50**, 725–732.

WEISBERG M. K., PRINZ M., and NEHRU C. E. (1988) Petrology of ALH85085: A chondrite with unique characteristics. *Earth Planet. Sci. Lett.* **91**, 19–32.

WIDGE S. and GOLDSTEIN J. I. (1977) Redetermination of the Fe-rich portion of the Fe-Ni-Co phase diagram. *Metal. Trans.* **8A**, 309–315.

WILLIAMS C. V., RUBIN A. E., KEIL K., and SAN MIGUEL A. (1985) Petrology of the Cangas de Onis and Nulles regolith breccias: Implications for parent body history. *Meteoritics* **20**, 331–345.

WILLIS J. and GOLDSTEIN J. I. (1981) Solidification zoning and metallographic cooling rates of chondrites. *Nature* **293**, 126–127.

WILLIS J. and GOLDSTEIN J. I. (1983) A three-dimensional study of metal grains in equilibrated, ordinary chondrites. *Proc. Lunar Planet. Sci. Conf. 14th*, B287–B292.

WOOD J. A. (1967) Chondrites: Their metallic minerals, thermal histories and parent planets. *Icarus* **6**, 1–49.

ZAVARITSKJI A. N. and KVASHA L. G. (1952) *Meteorites of the USSR* (in Russian). Kollektsia Akad., Nauka, Moscow.